Simulating the Effects of Atrial Fibrillation in Electrically Heterogeneous Human Atria: A Computer Modelling Study

J Stott, S Kharche, P Law, H Zhang

University of Manchester, Manchester, UK

Abstract

We postulated that atrial fibrillation (AF) induced electrical remodelling in electrically heterogeneous human atria facilitates chronic AF.

A modern biophysically detailed mathematical model of human atrial action potential was modified to incorporate electrophysiological properties of different cell types present within the atria. The heterogeneous cell models were then further modified to incorporate data on AF induced electrical remodelling (AFER) of ion channel kinetics and current densities. These modified models were used to simulate electrical activity in cells, 1D strands and 2D heterogeneous sheets.

AFER heterogeneously reduced action potential duration in all cell types. The theme of inhomogeneous response to AFER was observed through all cell and 1D simulations. Sheet simulations showed that whilst re-entry self terminated in the control case, it persisted under AFER conditions.

1. Introduction

The human atria consists of several tissue types each with distinct electrophysiological properties. It has previously been shown that inhomogeneity in tissues can lead to re-entrant activity [1–3]. There is also experimental data available on the ion channel remodelling due to atrial fibrillation induced remodelling (AFER) during chronic atrial fibrillation (AF) on human atrial cells [4, 5].

In this study, we quantified the changes in electrophysiological behavior in cell and 1D homogeneous models under AFER compared to control conditions. Further, reentrant waves in 2D electrically homogeneous and electrically heterogeneous sheets were studied.

2. Methods

The human atrial action potential (AP) model by Courtemanche et al. (CRN) [6] was used in this study. Modifications were incorporated to reproduce the differing APs of the different atrial cell types [7]. This produced distinct APs for the crista terminalis (CT), pectinate muscles (PM), atrio-ventricular ring bundle and the Bachmann bundle. Atrial myocyte (AM) cells were modelled by the original CRN model.

The data for AFER were taken from experiments by Bosch et al. [4] and Workman et al. [5], representing the changes in ion channels in patients after one month (AF1) and up to six months (AF2) of chronic AF, respectively. The modifications to the cellular electrophysiology were described in Kharche et al. [8].

Single cell behavior was quantified through a number of measures. Action potential duration (APD_{90}) was defined as the time after stimulation to 90 % re-polarisation of the 10^{th} AP in a train paced at a basic cycle length (BCL) of 1000 ms. APD_{90} restitution (APDr) was calculated using a standard S1–S2 protocol [8]. Effective refractory period restitution (ERPr) was calculated after [5]. BCLs ranging from 100 ms to 1000 ms were used for pre-pacing.

The electrical wave propagation was described via a partial differential equation (PDE) system with isotropic cell-to-cell conduction [9],

$$\frac{\partial V}{\partial t} = D\nabla^2 V - \frac{I_{ion}}{C_m} \quad (1)$$

where V is the membrane potential, t the time, D the diffusion co-efficient, ∇^2 the diffusion operator, I_{ion} the total trans-membrane current and C_m the membrane capacitance. In these simulations, I_{ion} was described by the CRN model, modified as previously described.

Homogeneous 1D strand models of AM, PM and CT cells were constructed to study the effect of AFER on conduction velocity (CV), maximal pacing rate and vulnerability window (VW) of tissue to creation of unidirectional

block, in response to a premature stimulus applied in the refractory tail of a previous excitation. The conduction velocity restitution (CVr) was computed via a standard protocol and the VW as described in [10]. Maximal pacing rate was determined from the closest pair of stimuli which produced excitation waves that travelled the length of the strand. The strands were 10 mm long with a spatial resolution of 0.1 mm. The diffusion constant, D, was set to 0.03125 mm^2ms^{-1} [11] to give a solitary wave CV of 0.27 mm ms^{-1} in a control AM strand.

Further, a 2D electrically heterogeneous sheet model was developed based on a laboratory photograph of the right atrium. The photograph was digitized at a spatial resolution of 0.1 mm. The model developed by segmenting areas of the tissue into AM, PM and CT tissue types. The complete model had a size of 130 x 100 mm and consisted of approximately 1 million active grid points.

The simulations were performed with all cells under control, AF1 and AF2 conditions, with the conditions applied uniformly to the tissue. All 2D sheet simulations were performed with the space step of 0.1 mm and a time step of 0.05 ms. A forward Euler scheme was used to advance the PDE, with selected channels advanced via the Rush-Larsen method [12]. Re-entry was induced in the centre of the tissue via a cross–field protocol [11].

The code utilized the OpenMP library for parallelization. All 2D simulations were executed on a Bull Itanium2 system. All 2D visualizations were carried out in-process using the libgif libraries.

3. Results

Simulations were performed for all three cases: control, AF1 and AF2. However the results for AF1 and AF2 were qualitatively similar, although AF1 showed a much more profound effect on APD_{90} reduction. Since the 2D preparation had no Bachmann bundle or atrio-ventricular ring cells present, the single cell and strand results do not show these cell types.

Incorporating the heterogeneity and AFER data causes significant differences in APD_{90} to manifest, as shown in Figure 1. The effects of AFER are not uniform across the different cell types of the atrium and it increases the difference in APD_{90} between normal atrial myocytes and the CT cells, increasing from 20.1 ms in control to 28.1 ms in AF1 and 33.4 ms in AF2.

The APDr curves, shown in Figure 1, are flatter over much of the range of diastolic intervals for AF1 and AF2 as compared to control. However, the maximal slopes of the APDr curves for CT cells are higher for AF1, 5.3, and AF2, 2.8, compared with 2.1 in control. The difference in the maximal slopes in different tissue types is increased, with CT having a larger maximal slope in all cases. In the control tissue, the difference in maximal slopes was 0.1,

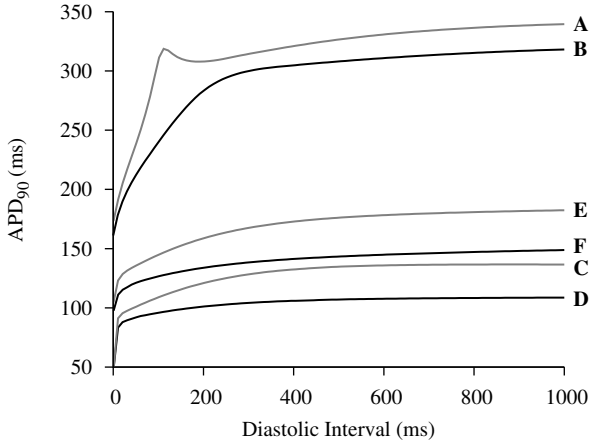

Figure 1. APDr curves for control CT (A), control AM/PM (B), AF1 CT (C), AF1 AM/PM (D), AF2 CT (E), AF2 AM/PM (F). In all cases the CT action potentials are above the AM/PM action potentials over the whole of the range considered.

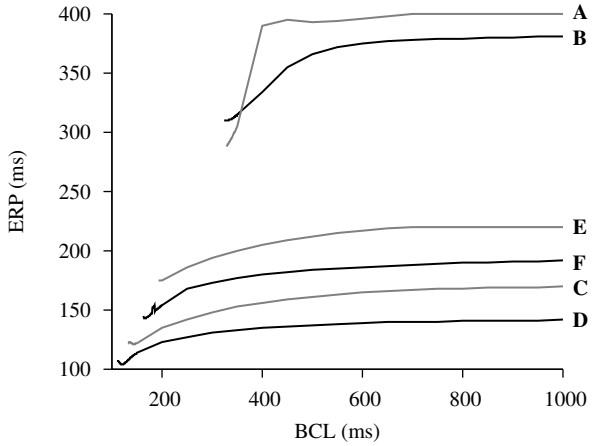

Figure 2. ERPr curves for control CT (A), control AM/PM (B), AF1 CT (C), AF1 AM/PM (D), AF2 CT (E), AF2 AM/PM (F). Both AF1 and AF2 have a significantly reduced ERPr over the whole range considered, with AF1 having a lower ERP then AF2. In addition, AF1 and AF2 cells are still excitable after pacing at 100 ms shorter BCL.

compared with 0.4 in AF1 and 0.5 in AF2 tissue.

In AF tissue, the ERPr was flattened for all tissue types compared with the control cells, as shown in Figure 2. This also allowed successful excitation at lower BCLs for AF tissue than was possible in control tissue. Heterogeneity in ERPr was largely unaffected by AF.

Conduction velocity, shown in Figure 3, was slowed by AF, reducing the solitary wave velocity from 0.27 mm ms^{-1} in control to 0.25 mm ms^{-1} in AF1 and 0.26 mm ms^{-1} in AF2. Maximal pacing rate increased from the control value of 198 bpm to 421 bpm in AF1

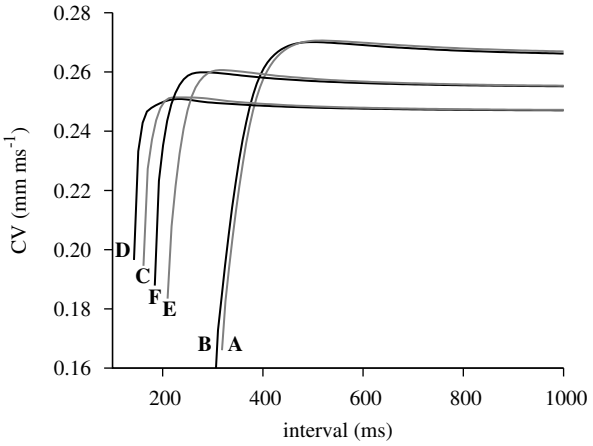

Figure 3. CVr curves for control CT (A), control AM/PM (B), AF1 CT (C), AF1 AM/PM (D), AF2 CT (E), AF2 AM/PM (F). In each of the conditions, the CT cells showed a higher CV at long (1000 ms) S2 intervals, but AM and PM cells allow faster conduction at shorter S2 intervals. The AF cases show reduced CV compared to the control and support a higher pacing rate via reduced minimum interval.

strands and 315 bpm in AF2 strands.

The VW was reduced by AF, but in all cell types the reduction was small. The control value of 16.6 ms was reduced to 14.2 ms in AF1 and 14.7 ms in AF2 for AM and PM cell types. The reduction in VW for CT cells was even smaller, from 15.1 ms in control to 14.5 ms and 14.4 ms in AF1 and AF2, respectively.

Simulations over the 2D geometry examined the lifetime and behavior of spiral waves in the presence and absence of electrical heterogeneity. As can be seen in Figure 4, panels Ai and Bi, re-entrant activity self-terminated in both homogeneous and heterogeneous cases when due to spiral wave meander over a large tissue region, it exits the tissue. Self-termination was much more rapid in the electrically heterogeneous case, taking 1.31 s, compared with 3.20 s in the homogeneous case.

Conversely, under AF conditions the re-entry persisted after it was induced for the whole period of the simulation, a lifespan of over 5 s. Under electrically homogeneous conditions, panels Aii and Aiii show a stable mother rotor rotating anti-clockwise in the tissue. But in heterogeneous conditions, as shown in panels Bii and Biii, a similar mother rotor to the homogeneous cases is visible towards the right of each frame. On the left of the frames, the rotor breaks up into multiple fibrillatory wavelets on the border of the heterogeneous regions, forming a complex and chaotic pattern of excitation.

4. Discussion and conclusions

AFER induces significant changes in the cellular electrophysiology that appear to affect rate dependent electrical activities. It helps to sustain re-entry, providing evidence to substantiate the hypothesis of "AF begets AF".

Considering first the single cell results, one of the most obvious effects is the striking reduction in the APD_{90} and repolarization properties. AFER abbreviated APD_{90} in AM cells by 66 % in AF1 and 53 % in AF2. Other work has already suggested why the increases shown in the maximal slope of the APDr can be pro-arrhythmic [13], as can the reduced ERP [14]. Our study suggested that reduction is not uniform across all cell types, which leads to an augmented heterogeneity.

The 1D strand results for the CV tell a similar story. AFER tissue forms a much better substrate for arrhythmic activity, supporting both a much higher maximal pacing rate and in addition, the reduction in conduction wavelength, to below half the control values. This allows a greater number of excitation waves to exist in the tissue at any one time.

The 2D simulations in the realistic sheet show a marked difference in re-entrant behavior between homogeneous and heterogeneous simulations. The homogeneous sheets show self-termination of re-entry in control tissue, whilst the reduced ERP and conduction wavelength allow the rotor to remain stable and persist for the duration of the simulation in AFER condtions. The heterogeneous sheet simulations, show spiral wave breakup, as observed in real tissue [3], in both control and AF simulations, possibly due to elevated plateau potentials and increased refractory period of the CT cells. Self-termination is still observed in control simulations and is more rapid than in homogeneous tissue.

It is still unclear about the pro- or anti-arrhythmogenic effects of electrical heterogeneity in the human atria. Self-termination is more rapid in the heterogeneous tissue for the control case, but despite AFER increasing the heterogeneity between tissue types, it doesn't lead to self termination of the re-entry. In fact, it leads to breakup of the spiral wave in the region of the heterogeneity, leading to a region of erratic propagations, as has been seen in experiment [3]. Further study, in both 3D geometries and physiological experiments, would be needed to elucidate the true effects of the heterogeneity.

Acknowledgements

This work was supported by EPSRC DTA studentships EP/P50158X/1 (JS) and EP/P502616/1 (PL) and a Wellcome trust grant WT/081809/Z/06/Z (SK).

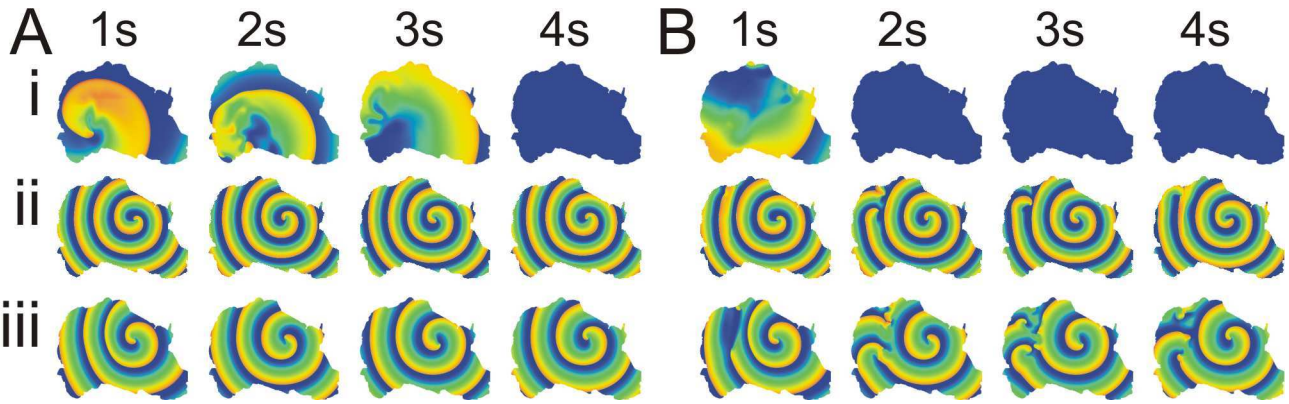

Figure 4. Simulation of re-entry in 2D sheets of electrically homogeneous (A) and electrically heterogeneous (B) sheets. Columns show representative frames after initiation of re-entry at t = 0. Panels i show data under control conditions, panels ii under AF1 conditions and panels iii under AF2 conditions. Re-entry self-terminated under control conditions in both homogeneous (Ai) and heterogeneous (Bi). Under AF conditions, re-entry becomes a sustained mother rotor in electrically homogeneous conditions (Aii, Aiii). However, under electrically heterogeneous conditions AF causes re-entry to degenerate into erratic propagations on the borders of the heterogeneity (Bii, Biii).

References

[1] Bernus O, Zemlin C, Zaritsky R, Minarov S, Pertsov A. Alternating conduction in the ischaemic border zone as a precursor of re-entrant arrhythmias: A simulation study. Europace 2005;7:S93–S104.

[2] Coronel R, Wilms-Schopman F, Opthof T, Fiolet J, Janse M. Reperfusion arrhythmias in isolated perfused pig hearts. inhomogeneities in extracellular potassium, st and tq potentials, and transmembrane action potentials. Circ Res 1992; 71(5):1131–1142.

[3] Kumagai K, Khrestian C, Waldo AL. Simultaneous multisite mapping studies during induced atrial fibrillation in the sterile pericarditis model. Insights into the mechanism of its maintenance. Circulation 1997;95(2):511–21.

[4] Bosch RF, Zeng X, Grammer JB, Popovic K, Mewis C, Kuhlkamp V. Ionic mechanisms of electrical remodeling in human atrial fibrillation. Cardiovasc Res 1999;44(1):121–31.

[5] Workman AJ, Kane KA, Rankin AC. The contribution of ionic currents to changes in refractoriness of human atrial myocytes associated with chronic atrial fibrillation. Cardiovasc Res 2001;52(2):226–35.

[6] Courtemanche M, Ramirez RJ, Nattel S. Ionic mechanisms underlying human atrial action potential properties: insights from a mathematical model. Am J Physiol 1998; 275:H301–21.

[7] Seemann G, Hoper C, Sachse FB, Dossel O, Holden AV, Zhang H. Heterogeneous three-dimensional anatomical and electrophysiological model of human atria. Philos Transact A Math Phys Eng Sci 2006;364(1843):1465–81.

[8] Kharche S, Seemann G, Leng J, Holden AV, Garratt CJ, Zhang H. Scroll waves in 3d virtual human atria: A computational study. In Sachse FB, Seemann G (eds.), FIMH 2007, volume 4466 of Lecture Notes in Computer Science. Springer, 2007; 129–138.

[9] Fenton F, Karma A. Vortex dynamics in three-dimensional continuous myocardium with fiber rotation: Filament instability and fibrillation. Chaos 1998;8(1):20–47.

[10] Zhang H, Holden AV. One-dimensional modelling of the vulnerability to re-entry of homogeneous atrial tissue. J Theor Biol 1997;184(2):117–22.

[11] Biktasheva IV, Biktashev VN, Holden AV. Wavebreaks and self-termination of spiral waves in a model of human atrial tissue. In Frangi AF, Radeva P, Santos A, Hernandez M (eds.), FIMH 2005, volume 3504 of Lecture Notes in Computer Science. Springer, 2005; 293–303.

[12] Rush S, Larsen H. A practical algorithm for solving dynamic membrane equations. IEEE Trans Biomed Eng 1978; 25(4):389–92.

[13] Kim BS, Kim YH, Hwang GS, Pak HN, Lee SC, Shim WJ, Oh DJ, Ro YM. Action potential duration restitution kinetics in human atrial fibrillation. J Am Coll Cardiol 2002; 39(8):1329–1336.

[14] Xie F, Qu Z, Garfinkel A, Weiss JN. Electrical refractory period restitution and spiral wave reentry in simulated cardiac tissue. Am J Physiol Heart Circ Physiol 2002; 283(1):H448–60.

Address for correspondence:

Jonathan Stott
School of Physics and Astronomy, University of Manchester, Manchester, M13 9PL, UK
jonathan.stott@postgrad.manchester.ac.uk